THE JOURNAL OF PHYSICAL CHEMISTRY LETTERS
A JOURNAL OF THE AMERICAN CHEMICAL SOCIETY

pubs.acs.org/JPCL

Letter

Excited-State Properties of Defected Halide Perovskite Quantum Dots: Insights from Computation

Carlos Mora Perez,* Dibyajyoti Ghosh, Oleg Prezhdo, Sergei Tretiak, and Amanda J. Neukirch*

Cite This: *J. Phys. Chem. Lett.* 2021, 12, 1005−1011

Read Online

ACCESS | Metrics & More | Article Recommendations | Supporting Information

ABSTRACT: $CsPbBr_3$ quantum dots (QDs) have been recently suggested for their application as bright green light-emitting diodes (LEDs); however, their optical properties are yet to be fully understood and characterized. In this work, we utilize time-dependent density functional theory to analyze the ground and excited states of the $CsPbBr_3$ clusters in the presence of various low formation energy vacancy defects. Our study finds that the QD perovskites retain their defect tolerance with limited perturbance to the simulated UV−vis spectra. The exception to this general trend is that Br vacancies must be avoided, as they cause molecular orbital localization, resulting in trap states and lower LED performance. Blinking will likely still plague $CsPbBr_3$ QDs, given that the charged defects critically perturb the spectra via red-shifting and lower absorbance. Our study provides insight into the tunability of $CsPbBr_3$ QDs optical properties by understanding the nature of the electronic excitations and guiding improved development for high-performance LEDs.

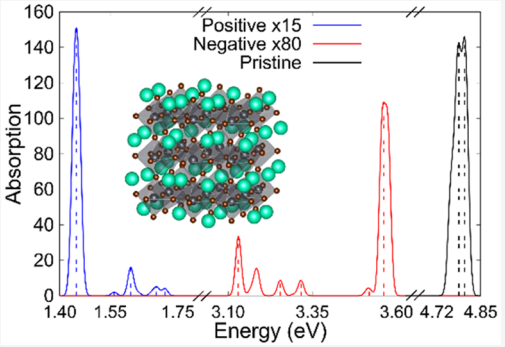

Lead halide perovskites (LHPs) have emerged as a unique material for various applications such as light-emitting diodes (LEDs),[1] photodetectors,[2] and solar cells[3,4] because of their facile synthesis,[5,6] convenient solution-based processing, and low fabrication cost.[7−10] More specifically, perovskite solar cells have undergone an 11% increase in cell efficiencies in only 6 years, currently reaching a remarkable 25.2% power conversion efficiency.[3,4] Meanwhile perovskite LEDs have increased to a photoluminescence quantum yield (PLQY) of ∼20% in 4 years,[11−14] further substantiating their promise as a possible candidate for high-performance optoelectronic devices. The general composition for a halide perovskite takes the form of ABX_3, where A is a cation (typically a small molecule such as methylammonium (MA) or formamidinium), B is a secondary cation (typically lead (Pb) or tin (Sn)), and X is a halogen (typically iodine(I), bromine (Br), or chlorine (Cl)). The most popular prototype is the hybrid organic−inorganic perovskite, $MAPbI_3$, which has remarkable optoelectronic properties.[15−17] However, more recently all-inorganic cesium LHP materials $CsPbX_3$ (X = Cl, Br, I) have taken center stage because of their higher thermal stability and lower degradation rate when exposed to air compared to that for hybrid perovskites.[18−26]

Given the promise shown by 3D bulk LHPs through extensive studies, the focus has eventually shifted to low-dimensional materials including two-dimensional (2D), one-dimensional (1D), and zero-dimensional (0D) systems.[27−33] Currently, significant effort has gone into the development and characterization of LHP quantum dots (QDs) (0D systems) with simple solution-based synthesis routes for LHP, such as $CsPbX_3$.[34,35] Similar to their 3D counterparts, LHP QDs have beneficial optoelectronic properties, such as narrow full width at half-maximum (FWHM) emission lines, high PLQY, and tunable band gaps.[36−38] These sustained properties allow for continued promising applications in solar cells (∼17% power conversion efficiency), LEDs (∼20% quantum yield), lasers, and displays.[39−42] Compared to its hybrid counterpart $MAPbX_3$, $CsPbX_3$ QDs have a more controllable diameter size and can easily achieve the full-spectrum light emission in the visible spectrum range and a high fluorescence quantum efficiency.[35,38,42] LHP LED devices are also boasted because of high mobility and increased color purity.[43,44] However, these QDs still suffer from the double-edge sword of solution-based synthesis: it allows for rapid and facile synthesis yet unfortunately results in unavoidable point defects.[45,46] Thus, it is critical to study the effects defects have on excited-state properties of perovskite QDs. $CsPbBr_3$ stands out as a favorable model for a QDs study due to a high PLQY (∼90%) with narrow FWHM superior to traditional CdSe-based QDs, enhanced color purity, excellent batch-to-batch reproducibility, and improvable thermal stability.[47−50]

Received: November 4, 2020
Accepted: January 12, 2021
Published: January 20, 2021

https://dx.doi.org/10.1021/acs.jpclett.0c03317
J. Phys. Chem. Lett. 2021, 12, 1005−1011

Although progress has been made into the characterizations of LHP QDs,[34,51−53] a thorough *ab initio* computational investigation into the ground- and excited-state properties of $CsPbBr_3$ QDs is still lacking. In these low-dimension materials, it is expected that photoluminescence (PL) originates from excitation recombination rather than bimolecular recombination.[54] Thus, understanding the nature of optical excitations and electronic structure can help to guide the tunability of the optoelectronic properties. This time-dependent density functional theory (TD-DFT) investigation focuses on $CsPbBr_3$ QDs in the presence of common low formation energy defects such as Cs, Br, and Pb vacancies as well as its charge states (+1, −1). Our systems were found to retain high-defect tolerance for most of the modeled defects. However, Br vacancies break this trend and severely affect the electronic structure, and thus it is imperative to avoid Br-deficient conditions thereby mitigating Br vacancies. Moreover, charge buildup will likely continue the blinking effect observed in other QD systems.

The charge-neutral pristine $CsPbBr_3$ perovskite nanocluster model under consideration is visualized in Figure 1a, with two

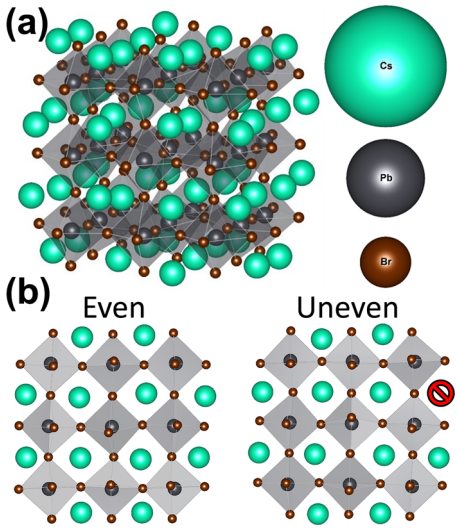

Figure 1. (a) Charge neutral pristine $CsPbBr_3$ nanocluster (3 × 3 × 3; 27-unit cell system), with Cs and Br terminated surface. (b) Unique surfaces of a cluster. The uneven surface natively contains a Cs vacancy.

unique terminated surfaces shown in Figure 1b (see the Methods section for more details). While our model system is smaller compared to experimentally investigated species because of the numerical cost involved in modeling large systems, we expect to have qualitatively similar excited-state features of both pristine QD and its defected counterparts.[55] We aim for a comprehensive computational investigation of this nanocrystal in the presence of various defects. Only charged vacancy defects are considered here to give a spin multiplicity of 1 required for spin-allowed singlet−singlet transitions. Table 1 provides a complete list of defects that we have considered in this study. These defects are chosen for their common appearance and low formation energy in bulk $CsPbBr_3$ perovskite material.[45,56,57] Specifically, halide defects have been shown time and again as the most readily produced defect with the lowest formation energy, which has the strongest effect on the electronic properties for $CsPbX_3$ perovskites.[45,56,57] Furthermore, we have also investigated

Table 1. Modeled Defect Types and Their Location on the $CsPbBr_3$ Nanocluster

Type	Location
Cs^{+1}	Even surface
	Uneven surface near native Cs vacancy 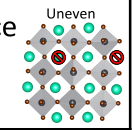
	Uneven surface far from native Cs vacancy 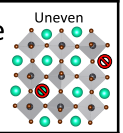
Pb^{+2}	Even surface
	Uneven surface
	Center "bulk like"
Br^{-1}	Even surface
	Uneven surface
+1	$[Cs_{54}Pb_{27}Br_{108}]^{+1}$
-1	$[Cs_{54}Pb_{27}Br_{108}]^{-1}$

charged systems in the form of a singly positively charged (+1) and negatively charged (−1) version of the neutral $CsPbBr_3$ QD as a way to probe the blinking effect commonly observed in semiconductor QDs.[58−60] This large array of defects allows us to properly review expected optical phenomena in perovskite QDs.

A common experimental method for probing low-lying energy states, such as the band gap, is ultraviolet−visible spectroscopy (UV−vis). The lowest energy peak (i.e., the band edge) observed in the UV−vis spectrum of a material can be approximated by the calculated energy gap (E_{HL}) being a difference between the highest occupied molecular orbital (HOMO)−lowest unoccupied molecular orbital (LUMO).[61] However, a more accurate representation would come from excited-state calculations typically done via TD-DFT methodology using hybrid functionals accounting for excitonic effects.[61,62] The Methods section outlines computational methodologies used in this work. The first step is to analyze optically allowed transitions. Given that the pristine and all vacancy-containing QDs have a singlet ground state, here we focus only on singlet−singlet transitions, assuming singlet-to-triplet transitions as optically forbidden (when neglecting spin−orbit interactions).

The UV−vis profile for the pristine $CsPbBr_3$ nanocluster composed of the first 15 singlet transitions is shown in Figure 2a with calculated band peaks at 4.78 and 4.80 eV. Experimental band gaps for 4 nm highly stable and reproducible QDs are around 2.75 eV.[63,64] Additionally, the smallest reported $CsPbBr_3$ based QDs are ∼1.1 nm with a more pronounced blue-shifted band gap of ∼2.86 eV.[65] Our nanoclusters having a cubic side length of ∼1.8 nm are within experimentally viable sizes. The higher energy band gaps that we report here are due to enhanced quantum confinement effects, given that considered nanoclusters are generally smaller than most experimentally stable sizes (greater than half in

https://dx.doi.org/10.1021/acs.jpclett.0c03317
J. Phys. Chem. Lett. 2021, 12, 1005−1011

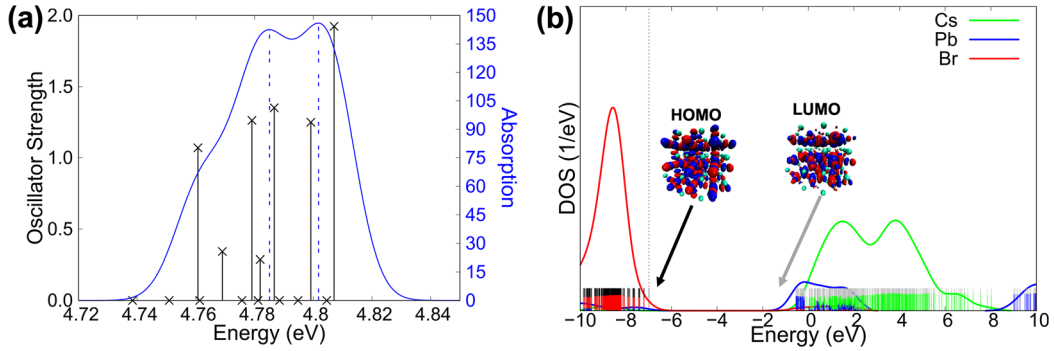

Figure 2. (a) Simulated UV−vis spectra of the pristine $CsPbBr_3$ nanocluster representing 15 singlet transitions. The oscillator strengths for the transitions are shown as black sticks capped with a cross (left scale). The resulting absorption profile is shown in the blue with the maximum peaks highlighted by a vertical dashed line (4.78 and 4.80 eV) (right scale). (b) Density of states (DOS) of the pristine system highlighting contributing atom types (here the vertical dashed line represents the HOMO level).

size), and our functional choice (here CAM-B3LYP model; see Methods section 1). The perturbative wave function methods such as ACD(2)/CC(2) may be employed to check the functional dependence of the band gap. While this may resolve uncertainty on the functional dependence in the TD-DFT approach for electronic transitions, we note that these methods carry a significantly higher computational cost for these methods, and there is a need to explore basis set dependence. This suggests a detailed future comparative study that needs to be performed for perovskite materials.

The blue-shift is caused by the quantum confinement effect which occurs when the QDs are smaller than the exciton Bohr radius of the material; namely, the $CsPbBr_3$ QDs has a reported Bohr radius of ~7 nm.[63,65−67] Thus, our small model size experiences a strong quantum confinement effects which significantly blue-shifts the band gap compared to available experimental data. Although macrotuning of the band gap is generally achieved from compositional engineering of the perovskite (i.e., changing the halide ion), the ability to fine-tune the band gap with cluster size is a positive feature of LHP QDs for blue LED candidates.[48,65,68]

Computed UV−vis profiles of the vacancy defect for Cs^{1+}, Pb^{2+}, and Br^{1-} are shown in Figure 3. The various Cs defects perturbed the spectra to a similar extent as seen by the overlapping UV−vis profiles which are red-shifted when compared to the first peak in the pristine system: Cs_{even} (Δ = −3.09 meV), $Cs_{far\ uneven}$ (Δ = −0.71 meV), and $Cs_{near\ uneven}$ (Δ = −3.41 meV). Although the individual transition peaks and oscillator strengths vary (see Supporting Information section 2), the overall profile remains largely unchanged. However, the break in the symmetry caused by the vacancies results in the oscillator strengths being controlled by the orbital overlap to a greater extent.[69] Pb defects have a more pronounced effect on the UV−vis profile, where the initial peaks differ as follows: Pb_{even} (Δ = −63.77 meV), Pb_{uneven} (Δ = −54.90 meV), and Pb_{Center} (Δ = −39.14 meV) (Figure 3b). The Pb vacancy on an even surface introduces the largest perturbation to the system as seen by the large red-shift in the initial band peak and by the absorption peak which is 2 times larger than that of the pristine system. The largest change to the UV−vis profile is due to Br vacancies on either surface; there is a large red-shift in the first band peak, Br_{even} (Δ = −566 meV) and Br_{uneven} (Δ = −582 meV) (Figure 3c). This is due to the lowering in the energy of the LUMO level caused by a strong spatial localization onto the vacancy site (see NTO/MO in Supporting Information section 4). Additionally, the Br

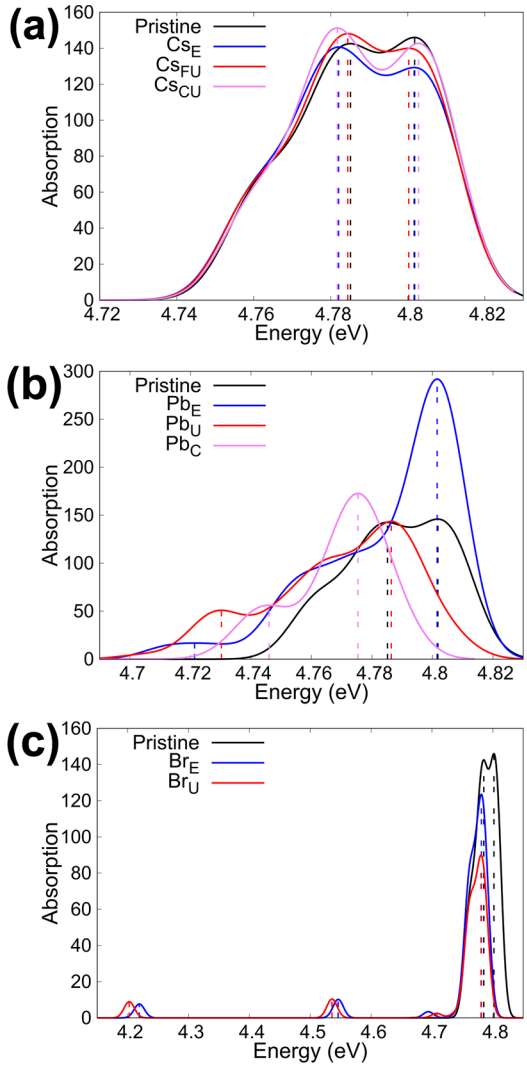

Figure 3. Simulated UV−vis spectra of the $CsPbBr_3$ nanocluster with defects calculated from the 15 lowest-energy singlet transitions: (a) Cs defects, (b) Pb defects, and (c) Br defects. Here "E" represents a defect from the even surface, and "U" represents a defect from the uneven surface (see Table 1 for defect locations).

vacancy creates shallow defect levels in the LUMO consistent with experimental bulk studies where halide vacancies create trap states near the conduction band.[45,56,57] As a continued

https://dx.doi.org/10.1021/acs.jpclett.0c03317
J. Phys. Chem. Lett. 2021, 12, 1005−1011

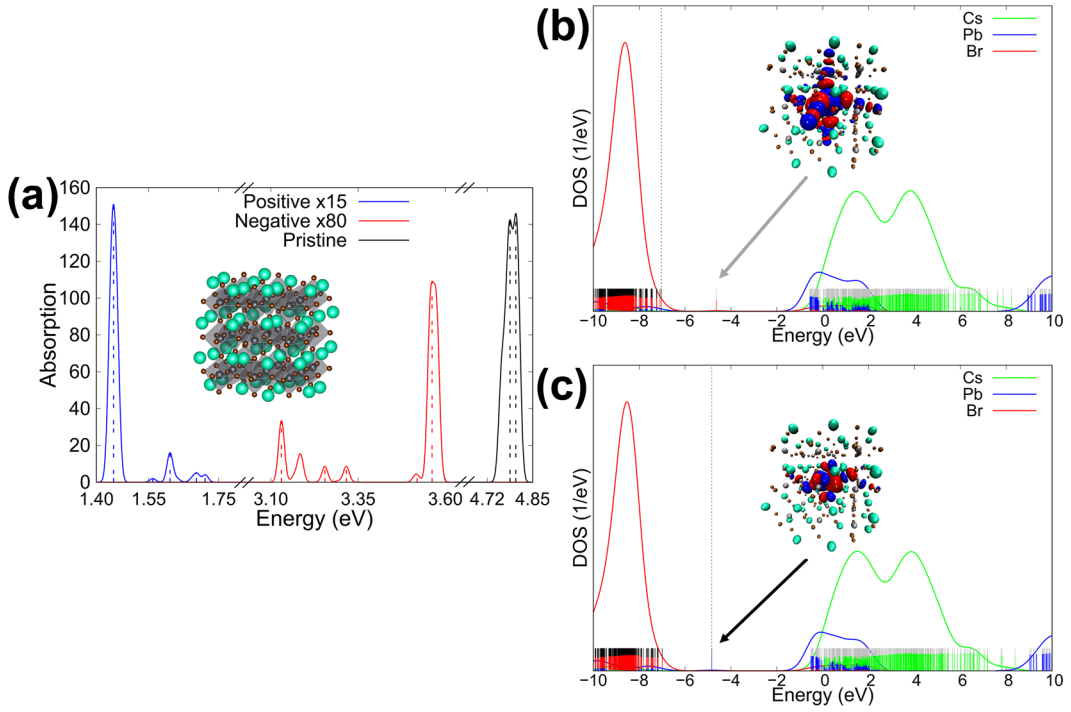

Figure 4. (a) UV−vis spectra comparison between the charged defects. (b) DOS of positively charged defect (resulting LUMO shown). (c) DOS of negatively charged defect (resulting HOMO shown).

testament to the extensively reported defect tolerance of $CsPbX_3$ perovskite materials,[45,57] the various vacancy defects have a minimal effect on the electronic properties of the systems, apart from the Br vacancies.

Given the trap states caused by the Br vacancies and lack of effect from Cs vacancies, it is best to synthesize these QD materials in a Br-rich/Cs-poor environment to reduce undesirable halide vacancies and promote increased performance.[57] Trap states allow for nonradiative pathways to dominate excitation radiative decay and reduce the desired device performance.[26] Although some of the modeled defects lead to trap states, their effect on the nonadiabatic electron−phonon coupling, decay, and dephasing times has yet to be studied. Thus, the rates of nonradiative decays cannot be accurately determined for the various modeled defects given the current computational scope. However, nonadiabatic molecular dynamic studies have been previously conducted on the parent $CsPbBr_3$ QD, which discusses methods for controlling the electron−hole recombination.[70−73] The optimal conditions of the bulk $CsPbBr_3$ and the formation energy of defects have been previously reported and completely align with our present results.[45,57] This alludes to the expected high performance of perovskite QDs for various photoluminescent applications.

Quantum dots as a class have been reported to provide a degraded performance when experiencing a blinking phenomenon, a fluctuation of photoluminescence (i.e., switching between active and dark states).[74−76] Blinking has been explained through the charging model in which the fluctuation is caused by photoionization and neutralization (i.e., a buildup of either positive or negative charge causes reduced photoluminescence).[74−76] This blinking effect can be probed by modeling an ionic system (i.e., a system with a single positive or negative charge) to provide insight into its continued effect on the newer perovskite QDs. The UV−vis profile comparison between the charge-neutral (pristine) and singly charged systems (positively and negatively charged ion system) is shown in Figure 4a. As expected, a charge buildup in the system causes lower oscillator strengths in the observed transitions; see individual transitions for charged systems in the Supporting Information section 2. The UV−vis profiles of the charged systems are 1 to 2 orders of magnitude lower than that of the neutral system, with the negative charge underperforming by a factor of 80 and the positive by a factor of 15. Note that both charged system spectra are significantly red-shifted compared to that for the pristine system. This can be attributed to the MO localization into the center of the system as seen in Figure 4b,c. For the positively charged system, the LUMO is a localized defect state and thus destabilizes the orbital which raises in energy when compared to the HOMO of the pristine system. In the negatively charged system, the HOMO is a localized defect state and thus stabilizes the orbital which lowers the energy when compared to the LUMO of the pristine system This localization and energy reordering of the orbitals result in a lower HOMO−LUMO gap of the charged states (see Figure 4b,c), which in turn affect the calculated UV−vis spectra. As the LUMO in the positive system is destabilized by 2.35 eV, while the HOMO in the negative system is stabilized by 4.28 eV, the positive system has a greater overall red-shift in the absorption profile. Thus, it is reasonable to expect blinking phenomena to be observed in photoluminescence of perovskite quantum dots unless charge stabilization would be achieved by, for instance, an appropriate shell of surface agents. Thus, the implementation of conventional mitigation strategies to reduce system charging of traditional QDs will continue to benefit the new LHP QDs.[77−79] Note that recent spectroscopic studies have extensively studied the excited-state charge distribution and dynamics.[80,81] These studies strongly suggest that charging of perovskite QDs can substantially affect their absorption and

https://dx.doi.org/10.1021/acs.jpclett.0c03317
J. Phys. Chem. Lett. 2021, 12, 1005−1011

emission profiles adversely. As we discussed here, our simulations provide in-depth reasoning of the charging effect at an atomistic level.

In summary, we have modeled several low-energy formation defects as well as charge buildup in the model LHP $CsPbBr_3$ nanocluster. True to its perovskite nature, our quantum dot was found to retain defect tolerance, with the exceptions of Br and charge defects. Therefore, defects that create localized electronic states resulting in shallow or deep level trap states open the system to nonradiative relaxation pathways.[54,75,76] These nonradiative pathways dictate the "on/off" behavior and lower photoluminescence. Consequently, it is vital to mitigate the low formation energy defects which cause the considered trap states in the material to optimize device performance. Particularly, one should avoid halide vacancies which can be reduced during the synthesis process in a halide-rich and/or Cs-poor environment. Alternatively, there have been several methods of surface passivation which improve charge carrier delocalization[79,82,83] and other methods that reduce vacancy concentration.[84,85] More generally, our results highlight properties of defects that can affect the performance of devices containing $CsPbBr_3$ nanoparticles.

■ ASSOCIATED CONTENT

Supporting Information

The Supporting Information is available free of charge at https://pubs.acs.org/doi/10.1021/acs.jpclett.0c03317.

Computational methodology; Figures S1−S12 (PDF)

■ AUTHOR INFORMATION

Corresponding Authors

Carlos Mora Perez − *Department of Chemistry, University of Southern California, Los Angeles, California 90089, United States; Theoretical Physics and Chemistry of Materials, Los Alamos National Laboratory, Los Alamos, New Mexico 87545, United States*; Email: morapere@usc.edu

Amanda J. Neukirch − *Theoretical Physics and Chemistry of Materials, Los Alamos National Laboratory, Los Alamos, New Mexico 87545, United States*; orcid.org/0000-0002-6583-0086; Email: ajneukirch@lanl.gov

Authors

Dibyajyoti Ghosh − *Theoretical Physics and Chemistry of Materials and Center for Nonlinear Studies, Los Alamos National Laboratory, Los Alamos, New Mexico 87545, United States*; orcid.org/0000-0002-3640-7537

Oleg Prezhdo − *Department of Chemistry, University of Southern California, Los Angeles, California 90089, United States*; orcid.org/0000-0002-5140-7500

Sergei Tretiak − *Theoretical Physics and Chemistry of Materials, Los Alamos National Laboratory, Los Alamos, New Mexico 87545, United States*; orcid.org/0000-0001-5547-3647

Complete contact information is available at: https://pubs.acs.org/10.1021/acs.jpclett.0c03317

Notes

The authors declare no competing financial interest.

■ ACKNOWLEDGMENTS

C.M.P., D.G., S.T., and A.J.N. acknowledge the LANL LDRD program. This work was done in part at the Center for Nonlinear Studies (CNLS) and the Center for Integrated Nanotechnologies (CINT), a U.S. Department of Energy and Office of Basic Energy Sciences user facility, at LANL. This research used resources provided by the LANL Institutional Computing Program. Los Alamos National Laboratory is operated by Triad National Security, LLC, for the National Nuclear Security Administration of the U.S. Department of Energy (Contract 89233218NCA000001). C.M.P. and O.V.P. acknowledge funding from the U.S. Department of Energy, Grant DE-SC0014429.

■ REFERENCES

(1) Era, M.; Morimoto, S.; Tsutsui, T.; Saito, S. Organic-inorganic Heterostructure Electroluminescent Device Using a Layered Perovskite Semiconductor $(C_6H_5C_2H_4NH^3)_2PbI_4$. *Appl. Phys. Lett.* **1994**, *65* (6), 676−678.

(2) Zhou, J.; Huang, J. Photodetectors Based on Organic-Inorganic Hybrid Lead Halide Perovskites. *Adv. Sci.* **2018**, *5* (1), 1700256.

(3) Yang, W. S.; Park, B.-W.; Jung, E. H.; Jeon, N. J.; Kim, Y. C.; Lee, D. U.; Shin, S. S.; Seo, J.; Kim, E. K.; Noh, J. H.; Seok, S. Il Iodide Management in Formamidinium-Lead-Halide-Based Perovskite Layers for Efficient Solar Cells. *Science* **2017**, *356* (6345), 1376−1379.

(4) Kojima, A.; Teshima, K.; Shirai, Y.; Miyasaka, T. Organometal Halide Perovskites as Visible-Light Sensitizers for Photovoltaic Cells. *J. Am. Chem. Soc.* **2009**, *131* (17), 6050−6051.

(5) Nguyen, T. P.; Ozturk, A.; Park, J.; Sohn, W.; Lee, T. H.; Jang, H. W.; Kim, S. Y. Facile Synthesis of $CsPbBr_3$/PbSe Composite Clusters. *Sci. Technol. Adv. Mater.* **2018**, *19* (1), 10−17.

(6) Hassan, Y.; Ashton, O. J.; Park, J. H.; Li, G.; Sakai, N.; Wenger, B.; Haghighirad, A.-A.; Noel, N. K.; Song, M. H.; Lee, B. R.; Friend, R. H.; Snaith, H. J. Facile Synthesis of Stable and Highly Luminescent Methylammonium Lead Halide Nanocrystals for Efficient Light Emitting Devices. *J. Am. Chem. Soc.* **2019**, *141* (3), 1269−1279.

(7) Lin, Q.; Armin, A.; Burn, P. L.; Meredith, P. Organohalide Perovskites for Solar Energy Conversion. *Acc. Chem. Res.* **2016**, *49* (3), 545−553.

(8) Zhao, Y.; Zhu, K. Solution Chemistry Engineering toward High-Efficiency Perovskite Solar Cells. *J. Phys. Chem. Lett.* **2014**, *5* (23), 4175−4186.

(9) Etgar, L.; Gao, P.; Xue, Z.; Peng, Q.; Chandiran, A. K.; Liu, B.; Nazeeruddin, M. K.; Grätzel, M. Mesoscopic $CH_3NH_3PbI_3/TiO_2$ Heterojunction Solar Cells. *J. Am. Chem. Soc.* **2012**, *134* (42), 17396−17399.

(10) Radicchi, E.; Mosconi, E.; Elisei, F.; Nunzi, F.; De Angelis, F. Understanding the Solution Chemistry of Lead Halide Perovskites Precursors. *ACS Appl. Energy Mater.* **2019**, *2* (5), 3400−3409.

(11) Chiba, T.; Hayashi, Y.; Ebe, H.; Hoshi, K.; Sato, J.; Sato, S.; Pu, Y.-J.; Ohisa, S.; Kido, J. Anion-Exchange Red Perovskite Quantum Dots with Ammonium Iodine Salts for Highly Efficient Light-Emitting Devices. *Nat. Photonics* **2018**, *12* (11), 681−687.

(12) Cho, H.; Jeong, S.-H.; Park, M.-H.; Kim, Y.-H.; Wolf, C.; Lee, C.-L.; Heo, J. H.; Sadhanala, A.; Myoung, N.; Yoo, S.; Im, S. H.; Friend, R. H.; Lee, T.-W. Overcoming the Electroluminescence Efficiency Limitations of Perovskite Light-Emitting Diodes. *Science* **2015**, *350* (6265), 1222−1225.

(13) Cao, Y.; Wang, N.; Tian, H.; Guo, J.; Wei, Y.; Chen, H.; Miao, Y.; Zou, W.; Pan, K.; He, Y.; Cao, H.; Ke, Y.; Xu, M.; Wang, Y.; Yang, M.; Du, K.; Fu, Z.; Kong, D.; Dai, D.; Jin, Y.; Li, G.; Li, H.; Peng, Q.; Wang, J.; Huang, W. Perovskite Light-Emitting Diodes Based on Spontaneously Formed Submicrometre-Scale Structures. *Nature* **2018**, *562* (7726), 249−253.

(14) Lin, K.; Xing, J.; Quan, L. N.; de Arquer, F. P. G.; Gong, X.; Lu, J.; Xie, L.; Zhao, W.; Zhang, D.; Yan, C.; Li, W.; Liu, X.; Lu, Y.; Kirman, J.; Sargent, E. H.; Xiong, Q.; Wei, Z. Perovskite Light-Emitting Diodes with External Quantum Efficiency Exceeding 20%. *Nature* **2018**, *562* (7726), 245−248.

(15) Wu, Y.; Xie, F.; Chen, H.; Yang, X.; Su, H.; Cai, M.; Zhou, Z.; Noda, T.; Han, L. Thermally Stable MAPbI3 Perovskite Solar Cells

with Efficiency of 19.19% and Area over 1 Cm^2 Achieved by Additive Engineering. *Adv. Mater.* **2017**, *29* (28), 1701073.
(16) Chen, Z.; Turedi, B.; Alsalloum, A. Y.; Yang, C.; Zheng, X.; Gereige, I.; AlSaggaf, A.; Mohammed, O. F.; Bakr, O. M. Single-Crystal MAPbI3 Perovskite Solar Cells Exceeding 21% Power Conversion Efficiency. *ACS Energy Lett.* **2019**, *4* (6), 1258−1259.
(17) Heo, J. H.; Han, H. J.; Kim, D.; Ahn, T. K.; Im, S. H. Hysteresis-Less Inverted $CH_3NH_3PbI_3$ Planar Perovskite Hybrid Solar Cells with 18.1% Power Conversion Efficiency. *Energy Environ. Sci.* **2015**, *8* (5), 1602−1608.
(18) Akbulatov, A. F.; Martynenko, V. M.; Frolova, L. A.; Dremova, N. N.; Zhidkov, I.; Tsarev, S. A.; Luchkin, S. Y.; Kurmaev, E. Z.; Aldoshin, S. M.; Stevenson, K. J.; Troshin, P. A. Intrinsic Thermal Decomposition Pathways of Lead Halide Perovskites $APbX_3$. *Sol. Energy Mater. Sol. Cells* **2020**, *213*, 110559.
(19) Thomas, C. J.; Zhang, Y.; Guillaussier, A.; Bdeir, K.; Aly, O. F.; Kim, H. G.; Noh, J.; Reimnitz, L. C.; Li, J.; Deepak, F. L.; Smilgies, D.-M.; Milliron, D. J.; Korgel, B. A. Thermal Stability of the Black Perovskite Phase in Cesium Lead Iodide Nanocrystals Under Humid Conditions. *Chem. Mater.* **2019**, *31* (23), 9750−9758.
(20) Leijtens, T.; Bush, K.; Cheacharoen, R.; Beal, R.; Bowring, A.; McGehee, M. D. Towards Enabling Stable Lead Halide Perovskite Solar Cells; Interplay between Structural, Environmental, and Thermal Stability. *J. Mater. Chem. A* **2017**, *5* (23), 11483−11500.
(21) He, Y.; Matei, L.; Jung, H. J.; McCall, K. M.; Chen, M.; Stoumpos, C. C.; Liu, Z.; Peters, J. A.; Chung, D. Y.; Wessels, B. W.; Wasielewski, M. R.; Dravid, V. P.; Burger, A.; Kanatzidis, M. G. High Spectral Resolution of Gamma-Rays at Room Temperature by Perovskite $CsPbBr_3$ Single Crystals. *Nat. Commun.* **2018**, *9* (1), 1609.
(22) Schlaus, A. P.; Spencer, M. S.; Miyata, K.; Liu, F.; Wang, X.; Datta, I.; Lipson, M.; Pan, A.; Zhu, X.-Y. How Lasing Happens in $CsPbBr_3$ Perovskite Nanowires. *Nat. Commun.* **2019**, *10* (1), 265.
(23) Wang, Y.; Dar, M. I.; Ono, L. K.; Zhang, T.; Kan, M.; Li, Y.; Zhang, L.; Wang, X.; Yang, Y.; Gao, X.; Qi, Y.; Grätzel, M.; Zhao, Y. Thermodynamically Stabilized β-CsPbI3-Based Perovskite Solar Cells with Efficiencies > 18%. *Science* **2019**, *365* (6453), 591−595.
(24) Steele, J. A.; Jin, H.; Dovgaliuk, I.; Berger, R. F.; Braeckevelt, T.; Yuan, H.; Martin, C.; Solano, E.; Lejaeghere, K.; Rogge, S. M. J.; Notebaert, C.; Vandezande, W.; Janssen, K. P. F.; Goderis, B.; Debroye, E.; Wang, Y.-K.; Dong, Y.; Ma, D.; Saidaminov, M.; Tan, H.; Lu, Z.; Dyadkin, V.; Chernyshov, D.; Van Speybroeck, V.; Sargent, E. H.; Hofkens, J.; Roeffaers, M. B. J. Thermal Unequilibrium of Strained Black CsPbI 3 Thin Films. *Science* **2019**, *365* (6454), 679−684.
(25) Swarnkar, A.; Marshall, A. R.; Sanehira, E. M.; Chernomordik, B. D.; Moore, D. T.; Christians, J. A.; Chakrabarti, T.; Luther, J. M. Quantum Dot-Induced Phase Stabilization of α-$CsPbI_3$ Perovskite for High-Efficiency Photovoltaics. *Science* **2016**, *354* (6308), 92−95.
(26) Li, W.; Long, R.; Tang, J.; Prezhdo, O. V. Influence of Defects on Excited-State Dynamics in Lead Halide Perovskites: Time-Domain Ab Initio Studies. *J. Phys. Chem. Lett.* **2019**, *10* (13), 3788−3804.
(27) Sanehira, E. M.; Marshall, A. R.; Christians, J. A.; Harvey, S. P.; Ciesielski, P. N.; Wheeler, L. M.; Schulz, P.; Lin, L. Y.; Beard, M. C.; Luther, J. M. Enhanced Mobility $CsPbI_3$ Quantum Dot Arrays for Record-Efficiency, High-Voltage Photovoltaic Cells. *Sci. Adv.* **2017**, *3* (10), No. eaao4204.
(28) Akkerman, Q. A.; Raino, G.; Kovalenko, M. V.; Manna, L. Genesis, Challenges and Opportunities for Colloidal Lead Halide Perovskite Nanocrystals. *Nat. Mater.* **2018**, *17* (5), 394−405.
(29) Kovalenko, M. V.; Protesescu, L.; Bodnarchuk, M. I. Properties and Potential Optoelectronic Applications of Lead Halide Perovskite Nanocrystals. *Science* **2017**, *358* (6364), 745−750.
(30) Li, X.; Cao, F.; Yu, D.; Chen, J.; Sun, Z.; Shen, Y.; Zhu, Y.; Wang, L.; Wei, Y.; Wu, Y.; Zeng, H. All Inorganic Halide Perovskites Nanosystem: Synthesis, Structural Features, Optical Properties and Optoelectronic Applications. *Small* **2017**, *13* (9), 1603996.
(31) Ghosh, D.; Acharya, D.; Pedesseau, L.; Katan, C.; Even, J.; Tretiak, S.; Neukirch, A. J. Charge Carrier Dynamics in Two-Dimensional Hybrid Perovskites: Dion-Jacobson vs. Ruddlesden-Popper Phases. *J. Mater. Chem. A* **2020**, *8*, 22009.
(32) Leveillee, J.; Katan, C.; Even, J.; Ghosh, D.; Nie, W.; Mohite, A. D.; Tretiak, S.; Schleife, A.; Neukirch, A. J. Tuning Electronic Structure in Layered Hybrid Perovskites with Organic Spacer Substitution. *Nano Lett.* **2019**, *19* (12), 8732−8740.
(33) Ghosh, D.; Neukirch, A. J.; Tretiak, S. Optoelectronic Properties of Two-Dimensional Bromide Perovskites: Influences of Spacer Cations. *J. Phys. Chem. Lett.* **2020**, *11* (8), 2955−2964.
(34) Chiba, T.; Kido, J. Lead Halide Perovskite Quantum Dots for Light-Emitting Devices. *J. Mater. Chem. C* **2018**, *6* (44), 11868−11877.
(35) Wei, Y.; Cheng, Z.; Lin, J. An Overview on Enhancing the Stability of Lead Halide Perovskite Quantum Dots and Their Applications in Phosphor-Converted LEDs. *Chem. Soc. Rev.* **2019**, *48* (1), 310−350.
(36) Chen, F.; Lin, Q.; Shen, H.; Tang, A. Blue Quantum Dot-Based Electroluminescent Light-Emitting Diodes. *Mater. Chem. Front.* **2020**, *4* (5), 1340−1365.
(37) Lao, X.; Li, X.; Ågren, H.; Chen, G. Highly Controllable Synthesis and DFT Calculations of Double/Triple-Halide CsPbX (X = Cl, Br, I) Perovskite Quantum Dots: Application to Light-Emitting Diodes. *Nanomaterials* **2019**, *9* (2), 172.
(38) Song, J.; Li, J.; Li, X.; Xu, L.; Dong, Y.; Zeng, H. Quantum Dot Light-Emitting Diodes Based on Inorganic Perovskite Cesium Lead Halides ($CsPbX_3$). *Adv. Mater.* **2015**, *27* (44), 7162−7167.
(39) Zhao, Q.; Hazarika, A.; Chen, X.; Harvey, S. P.; Larson, B. W.; Teeter, G. R.; Liu, J.; Song, T.; Xiao, C.; Shaw, L.; Zhang, M.; Li, G.; Beard, M. C.; Luther, J. M. High Efficiency Perovskite Quantum Dot Solar Cells with Charge Separating Heterostructure. *Nat. Commun.* **2019**, *10* (1), 2842.
(40) Li, F.; Zhou, S.; Yuan, J.; Qin, C.; Yang, Y.; Shi, J.; Ling, X.; Li, Y.; Ma, W. Perovskite Quantum Dot Solar Cells with 15.6% Efficiency and Improved Stability Enabled by an α-$CsPbI_3$/$FAPbI_3$ Bilayer Structure. *ACS Energy Lett.* **2019**, *4* (11), 2571−2578.
(41) Xiao, Z.; Kerner, R. A.; Zhao, L.; Tran, N. L.; Lee, K. M.; Koh, T.-W.; Scholes, G. D.; Rand, B. P. Efficient Perovskite Light-Emitting Diodes Featuring Nanometre-Sized Crystallites. *Nat. Photonics* **2017**, *11* (2), 108−115.
(42) Ning, Z.; Gong, X.; Comin, R.; Walters, G.; Fan, F.; Voznyy, O.; Yassitepe, E.; Buin, A.; Hoogland, S.; Sargent, E. H. Quantum-Dot-in-Perovskite Solids. *Nature* **2015**, *523* (7560), 324−328.
(43) Liang, H.; Yuan, F.; Johnston, A.; Gao, C.; Choubisa, H.; Gao, Y.; Wang, Y.-K.; Sagar, L. K.; Sun, B.; Li, P.; Bappi, G.; Chen, B.; Li, J.; Wang, Y.; Dong, Y.; Ma, D.; Gao, Y.; Liu, Y.; Yuan, M.; Saidaminov, M. I.; Hoogland, S.; Lu, Z.-H.; Sargent, E. H. High Color Purity Lead-Free Perovskite Light-Emitting Diodes via Sn Stabilization. *Adv. Sci.* **2020**, *7* (8), 1903213.
(44) Khan, Q.; Subramanian, A.; Yu, G.; Maaz, K.; Li, D.; Sagar, R. U. R.; Chen, K.; Lei, W.; Shabbir, B.; Zhang, Y. Structure Optimization of Perovskite Quantum Dot Light-Emitting Diodes. *Nanoscale* **2019**, *11* (11), 5021−5029.
(45) Zheng, X.; Hou, Y.; Sun, H.-T.; Mohammed, O. F.; Sargent, E. H.; Bakr, O. M. Reducing Defects in Halide Perovskite Nanocrystals for Light-Emitting Applications. *J. Phys. Chem. Lett.* **2019**, *10* (10), 2629−2640.
(46) Wang, F.; Bai, S.; Tress, W.; Hagfeldt, A.; Gao, F. Defects Engineering for High-Performance Perovskite Solar Cells. *npj Flex. Electron.* **2018**, *2* (1), 22.
(47) Swarnkar, A.; Chulliyil, R.; Ravi, V. K.; Irfanullah, M.; Chowdhury, A.; Nag, A. Colloidal CsPbBr3 Perovskite Nanocrystals: Luminescence beyond Traditional Quantum Dots. *Angew. Chem., Int. Ed.* **2015**, *54* (51), 15424−15428.
(48) Protesescu, L.; Yakunin, S.; Bodnarchuk, M. I.; Krieg, F.; Caputo, R.; Hendon, C. H.; Yang, R. X.; Walsh, A.; Kovalenko, M. V. Nanocrystals of Cesium Lead Halide Perovskites ($CsPbX_3$, X = Cl, Br, and I): Novel Optoelectronic Materials Showing Bright Emission with Wide Color Gamut. *Nano Lett.* **2015**, *15* (6), 3692−3696.
(49) Li, Z.; Kong, L.; Huang, S.; Li, L. Highly Luminescent and Ultrastable CsPbBr3 Perovskite Quantum Dots Incorporated into a

https://dx.doi.org/10.1021/acs.jpclett.0c03317
J. Phys. Chem. Lett. 2021, 12, 1005−1011

Silica/Alumina Monolith. *Angew. Chem., Int. Ed.* **2017**, *56* (28), 8134−8138.
(50) Sasaki, H.; Kamata, N.; Honda, Z.; Yasuda, T. Improved Thermal Stability of CsPbBr3 Quantum Dots by Ligand Exchange and Their Application to Light-Emitting Diodes. *Appl. Phys. Express* **2019**, *12* (3), 035004.
(51) Guijarro, N.; Yao, L.; Le Formal, F.; Wells, R. A.; Liu, Y.; Darwich, B. P.; Navratilova, L.; Cho, H.-H.; Yum, J.-H.; Sivula, K. Lead Halide Perovskite Quantum Dots To Enhance the Power Conversion Efficiency of Organic Solar Cells. *Angew. Chem., Int. Ed.* **2019**, *58* (36), 12696−12704.
(52) Kumar, S.; Jagielski, J.; Marcato, T.; Solari, S. F.; Shih, C.-J. Understanding the Ligand Effects on Photophysical, Optical, and Electroluminescent Characteristics of Hybrid Lead Halide Perovskite Nanocrystal Solids. *J. Phys. Chem. Lett.* **2019**, *10* (24), 7560−7567.
(53) Hosokawa, H.; Tamaki, R.; Sawada, T.; Okonogi, A.; Sato, H.; Ogomi, Y.; Hayase, S.; Okada, Y.; Yano, T. Solution-Processed Intermediate-Band Solar Cells with Lead Sulfide Quantum Dots and Lead Halide Perovskites. *Nat. Commun.* **2019**, *10* (1), 43.
(54) Nirmal, M.; Brus, L. Luminescence Photophysics in Semiconductor Nanocrystals. *Acc. Chem. Res.* **1999**, *32* (5), 407−414.
(55) Kilina, S.; Kilin, D.; Tretiak, S. Light-Driven and Phonon-Assisted Dynamics in Organic and Semiconductor Nanostructures. *Chem. Rev.* **2015**, *115* (12), 5929−5978.
(56) Sebastian, M.; Peters, J. A.; Stoumpos, C. C.; Im, J.; Kostina, S. S.; Liu, Z.; Kanatzidis, M. G.; Freeman, A. J.; Wessels, B. W. Excitonic Emissions and Above-Band-Gap Luminescence in the Single-Crystal Perovskite Semiconductors CsPbBr and CsPbCl. *Phys. Rev. B: Condens. Matter Mater. Phys.* **2015**, *92* (23), 235210.
(57) Kang, J.; Wang, L.-W. High Defect Tolerance in Lead Halide Perovskite CsPbBr3. *J. Phys. Chem. Lett.* **2017**, *8* (2), 489−493.
(58) Gibson, N. A.; Koscher, B. A.; Alivisatos, A. P.; Leone, S. R. Excitation Intensity Dependence of Photoluminescence Blinking in $CsPbBr_3$ Perovskite Nanocrystals. *J. Phys. Chem. C* **2018**, *122* (22), 12106−12113.
(59) Park, Y.-S.; Guo, S.; Makarov, N. S.; Klimov, V. I. Room Temperature Single-Photon Emission from Individual Perovskite Quantum Dots. *ACS Nano* **2015**, *9* (10), 10386−10393.
(60) Trinh, C. T.; Minh, D. N.; Ahn, K. J.; Kang, Y.; Lee, K.-G. Organic-Inorganic $FAPbBr_3$ Perovskite Quantum Dots as a Quantum Light Source: Single-Photon Emission and Blinking Behaviors. *ACS Photonics* **2018**, *5* (12), 4937−4943.
(61) Altaf, A. A.; Kausar, S.; Badshah, A. Spectral Calculations with DFT. In *Density Functional Calculations*; Yang, G., Ed.; IntechOpen: Rijeka, 2018.
(62) Casida, M. E.; Huix-Rotllant, M. Progress in Time-Dependent Density-Functional Theory. *Annu. Rev. Phys. Chem.* **2012**, *63* (1), 287−323.
(63) Dong, Y.; Qiao, T.; Kim, D.; Parobek, D.; Rossi, D.; Son, D. H. Precise Control of Quantum Confinement in Cesium Lead Halide Perovskite Quantum Dots via Thermodynamic Equilibrium. *Nano Lett.* **2018**, *18* (6), 3716−3722.
(64) Butkus, J.; Vashishtha, P.; Chen, K.; Gallaher, J. K.; Prasad, S. K. K.; Metin, D. Z.; Laufersky, G.; Gaston, N.; Halpert, J. E.; Hodgkiss, J. M. The Evolution of Quantum Confinement in $CsPbBr_3$ Perovskite Nanocrystals. *Chem. Mater.* **2017**, *29* (8), 3644−3652.
(65) Yang, H.; Feng, Y.; Tu, Z.; Su, K.; Fan, X.; Liu, B.; Shi, Z.; Zhang, Y.; Zhao, C.; Zhang, B. Blue Emitting $CsPbBr_3$ Perovskite Quantum Dot Inks Obtained from Sustained Release Tablets. *Nano Res.* **2019**, *12* (12), 3129−3134.
(66) Chen, H.; Guo, A.; Zhu, J.; Cheng, L.; Wang, Q. Tunable Photoluminescence of $CsPbBr_3$ Perovskite Quantum Dots for Their Physical Research. *Appl. Surf. Sci.* **2019**, *465*, 656−664.
(67) Kumawat, N. K.; Liu, X.-K.; Kabra, D.; Gao, F. Blue Perovskite Light-Emitting Diodes: Progress, Challenges and Future Directions. *Nanoscale* **2019**, *11* (5), 2109−2120.
(68) Zhao, Q.; Hazarika, A.; Schelhas, L. T.; Liu, J.; Gaulding, E. A.; Li, G.; Zhang, M.; Toney, M. F.; Sercel, P. C.; Luther, J. M. Size-Dependent Lattice Structure and Confinement Properties in $CsPbI_3$ Perovskite Nanocrystals: Negative Surface Energy for Stabilization. *ACS Energy Lett.* **2020**, *5* (1), 238−247.
(69) Atkins, P. W.; Friedman, R. S. *Molecular Quantum Mechanics*; OUP: Oxford, 2011.
(70) He, J.; Vasenko, A. S.; Long, R.; Prezhdo, O. V. Halide Composition Controls Electron-Hole Recombination in Cesium-Lead Halide Perovskite Quantum Dots: A Time Domain Ab Initio Study. *J. Phys. Chem. Lett.* **2018**, *9* (8), 1872−1879.
(71) Wang, S.; Luo, Q.; Fang, W.-H.; Long, R. Interfacial Engineering Determines Band Alignment and Steers Charge Separation and Recombination at an Inorganic Perovskite Quantum Dot/WS2 Junction: A Time Domain Ab Initio Study. *J. Phys. Chem. Lett.* **2019**, *10* (6), 1234−1241.
(72) Zhang, Z.; He, J.; Long, R. Ultrafast Charge Separation and Recombination across a Molecule/$CsPbBr_3$ Quantum Dot Interface from First-Principles Nonadiabatic Molecular Dynamics Simulation. *J. Phys. Chem. C* **2019**, *123* (39), 23800−23806.
(73) Qiao, L.; Fang, W.-H.; Long, R.; Prezhdo, O. V. Photoinduced Dynamics of Charge Carriers in Metal Halide Perovskites from an Atomistic Perspective. *J. Phys. Chem. Lett.* **2020**, *11* (17), 7066−7082.
(74) Frantsuzov, P.; Kuno, M.; Jankó, B.; Marcus, R. A. Universal Emission Intermittency in Quantum Dots, Nanorods and Nanowires. *Nat. Phys.* **2008**, *4* (7), 519−522.
(75) Galland, C.; Ghosh, Y.; Steinbrück, A.; Sykora, M.; Hollingsworth, J. A.; Klimov, V. I.; Htoon, H. Two Types of Luminescence Blinking Revealed by Spectroelectrochemistry of Single Quantum Dots. *Nature* **2011**, *479* (7372), 203−207.
(76) Yuan, G.; Gómez, D. E.; Kirkwood, N.; Boldt, K.; Mulvaney, P. Two Mechanisms Determine Quantum Dot Blinking. *ACS Nano* **2018**, *12* (4), 3397−3405.
(77) Seth, S.; Ahmed, T.; Samanta, A. Photoluminescence Flickering and Blinking of Single CsPbBr3 Perovskite Nanocrystals: Revealing Explicit Carrier Recombination Dynamics. *J. Phys. Chem. Lett.* **2018**, *9* (24), 7007−7014.
(78) Sharma, D. K.; Hirata, S.; Vacha, M. Single-Particle Electroluminescence of $CsPbBr_3$ Perovskite Nanocrystals Reveals Particle-Selective Recombination and Blinking as Key Efficiency Factors. *Nat. Commun.* **2019**, *10* (1), 4499.
(79) Chen, Y.; Vela, J.; Htoon, H.; Casson, J. L.; Werder, D. J.; Bussian, D. A.; Klimov, V. I.; Hollingsworth, J. A. Giant" Multishell CdSe Nanocrystal Quantum Dots with Suppressed Blinking. *J. Am. Chem. Soc.* **2008**, *130* (15), 5026−5027.
(80) Nakahara, S.; Ohara, K.; Tahara, H.; Yumoto, G.; Kawawaki, T.; Saruyama, M.; Sato, R.; Teranishi, T.; Kanemitsu, Y. Ionization and Neutralization Dynamics of $CsPbBr_3$ Perovskite Nanocrystals Revealed by Double-Pump Transient Absorption Spectroscopy. *J. Phys. Chem. Lett.* **2019**, *10* (16), 4731−4736.
(81) Soetan, N.; Puretzky, A.; Reid, K.; Boulesbaa, A.; Zarick, H. F.; Hunt, A.; Rose, O.; Rosenthal, S.; Geohegan, D. B.; Bardhan, R. Ultrafast Spectral Dynamics of $CsPb(BrxCl_{1-x})_3$ Mixed-Halide Nanocrystals. *ACS Photonics* **2018**, *5* (9), 3575−3583.
(82) Vickers, E. T.; Graham, T. A.; Chowdhury, A. H.; Bahrami, B.; Dreskin, B. W.; Lindley, S.; Naghadeh, S. B.; Qiao, Q.; Zhang, J. Z. Improving Charge Carrier Delocalization in Perovskite Quantum Dots by Surface Passivation with Conductive Aromatic Ligands. *ACS Energy Lett.* **2018**, *3* (12), 2931−2939.
(83) Xue, J.; Wang, R.; Yang, Y. The Surface of Halide Perovskites from Nano to Bulk. *Nat. Rev. Mater.* **2020**, *5*, 809.
(84) Zheng, X.; Troughton, J.; Gasparini, N.; Lin, Y.; Wei, M.; Hou, Y.; Liu, J.; Song, K.; Chen, Z.; Yang, C.; Turedi, B.; Alsalloum, A. Y.; Pan, J.; Chen, J.; Zhumekenov, A. A.; Anthopoulos, T. D.; Han, Y.; Baran, D.; Mohammed, O. F.; Sargent, E. H.; Bakr, O. M. Quantum Dots Supply Bulk- and Surface-Passivation Agents for Efficient and Stable Perovskite Solar Cells. *Joule* **2019**, *3* (8), 1963−1976.
(85) Liu, S.-C.; Li, Z.; Yang, Y.; Wang, X.; Chen, Y.-X.; Xue, D.-J.; Hu, J.-S. Investigation of Oxygen Passivation for High-Performance All-Inorganic Perovskite Solar Cells. *J. Am. Chem. Soc.* **2019**, *141* (45), 18075−18082.

https://dx.doi.org/10.1021/acs.jpclett.0c03317
J. Phys. Chem. Lett. 2021, 12, 1005−1011